

Arterial Branching within the Confines of Fractal L-System Formalism

M. ZAMIR

Department of Applied Mathematics and Department of Medical Biophysics, University of Western Ontario, London, N6A 5B7, Canada

ABSTRACT Parametric Lindenmayer systems (L-systems) are formulated to generate branching tree structures that can incorporate the physiological laws of arterial branching. By construction, the generated trees are de facto fractal structures, and with appropriate choice of parameters, they can be made to exhibit some of the branching patterns of arterial trees, particularly those with a preponderant value of the asymmetry ratio. The question of whether arterial trees in general have these fractal characteristics is examined by comparison of pattern with vasculature from the cardiovascular system. The results suggest that parametric L-systems can be used to produce fractal tree structures but not with the variability in branching parameters observed in arterial trees. These parameters include the asymmetry ratio, the area ratio, branch diameters, and branching angles. The key issue is that the source of variability in these parameters is not known and, hence, it cannot be accurately reproduced in a model. L-systems with a random choice of parameters can be made to mimic some of the observed variability, but the legitimacy of that choice is not clear.

KEY WORDS: arterial tree • L-system • branching • self-similarity • vasculature

INTRODUCTION

The branching structure of vascular systems has been the subject of much discussion and debate since it was first suggested that these systems may have fractal architecture (Mandelbrot, 1977). The great variety of vascular systems in biology, and the apparent similarity between the branching structure of such diverse systems as blood arteries (Murray, 1926a,b), botanical plants (Prusinkiewicz and Lindenmayer, 1990), neural systems (Berry and Pymm, 1981), and rivers (Horton, 1945), make the subject somewhat intractable when it comes to the study of form as it relates to function. For a meaningful discussion, the subject must clearly be narrowed. In this paper, the focus is on arterial systems associated with hemodynamics primarily in mammals.

There is no doubt that even here the entire spectrum of vascular systems cannot be treated in the same way. The vascular system of the kidney (Moffat, 1979), for example, serves a filtration function in which the number of branches and ultimate filtration units is important but their location is not. The same can be said of the lung's airways and pulmonary arteries, the ultimate functional units in this case being the alveoli where oxygen exchange takes place (Weibel, 1984). In the core of the systemic arterial system, on the other hand, the main business of vasculature is to reach certain organs or destinations within the body and to bring blood supply to these destinations in appropriate quantities. An-

other system of vessels within each organ or destination then does the same on a smaller scale. In these systems, the distribution of branches and subbranches is highly nonuniform because it is determined by reasons of anatomy and local flow requirements (Fig. 1). By contrast, in the lungs and kidneys, the functional units are packed neatly together and the required vasculature is set in a fairly uniform manner (Fig. 2).

These considerations suggest that discussion of fractal properties of vascular systems, if it is to relate to function, should be limited to particular categories of systems rather than collectively to all. In this paper, the focus is on arterial systems in the systemic circulation whose main function is the distribution and delivery of blood, rather than filtration or other processing functions. These systems are found to have a predominantly open tree structure and include large and small vessels up to, but not including, the capillary bed. Capillary beds are not included because they are of a different category and their branching structure, characterized by interconnections and closed loops, requires separate treatment (Weibel, 1984).

The term "arterial tree" shall be used generically to mean the branching structure of a main artery in the systemic circulation from its source to its final branches as they reach the capillary bed, but not including the latter. It may represent the aorta from its origin at the left ventricle and include its entire distribution or a smaller system such as that of a coronary artery. It has been found that these and other arterial trees in the systemic circulation have an open tree structure based on repeated bifurcations. This structure is a fractal

Address correspondence to Dr. M. Zamir, Department of Applied Mathematics, University of Western Ontario, London, Ontario, N6A 5B7, Canada. Fax: (519) 661-3523; E-mail: zamir@uwo.ca.

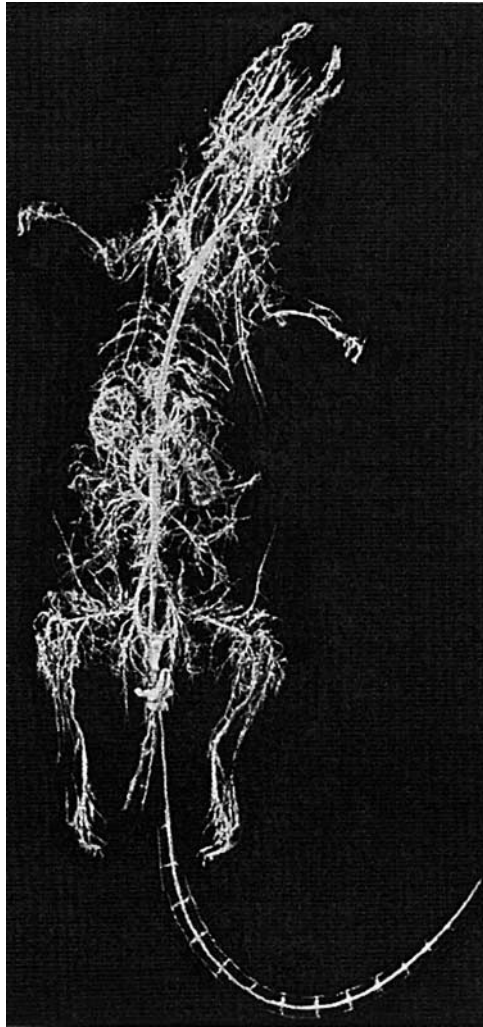


FIGURE 1. A reasonably complete cast of the arterial system of a rat (Zamir et al., 1983). Branching is highly nonuniform and is dictated by reasons of anatomy, local flow requirements, and other constraints.

structure in the sense that each level of the tree is obtained from that preceding it by dichotomous division. However, in the context of physiology, this fractal character is not useful unless the dichotomous divisions are allowed to have the range of properties that arterial bifurcations in the cardiovascular system are known to have (Zamir, 1999). These properties include relations between diameters of the three vessels involved at an arterial bifurcation and the angles that the two branches make with the direction of the parent vessel. The object of this paper is to incorporate these properties into a so-called parametric L-system to produce open tree structures that are both fractal in character and physiological in their branching properties.

MATERIALS AND METHODS

The fractal properties of an arterial tree may be discussed in terms of its "fractal dimension" (Peitgen et al., 1992), which in

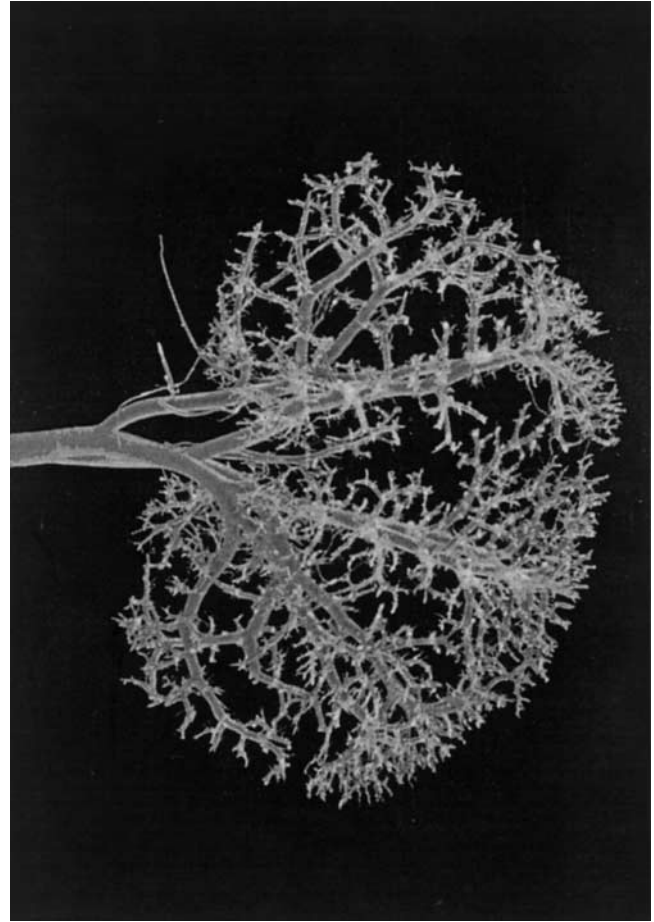


FIGURE 2. A close up of the vasculature of the kidney, from a cast of the arterial system of a rat (Zamir and Phipps, 1987. By permission of NRC Research Press). The branching pattern appears more uniform overall, but on the local scale of individual bifurcations there is considerable variability in the size and angle of branches. This suggests that variability is present even when vasculature is free to develop in a strictly uniform pattern as it is in this case.

turn may be defined in terms of some power law progression of a functional or geometrical property along the tree such as flow rate, velocity, branch length, or diameter. This method has met with some difficulty because it is usually based on the assumption of symmetrical and uniform branching at all levels of the tree. Data from the arterial tree (Zamir and Brown, 1982) indicate considerable nonsymmetry and nonuniformity. Fractal dimension can also be defined by the so-called "box-counting" method, which essentially determines the space-filling property of the tree (Peitgen et al., 1992). The difficulty with this method for the present purpose is that it does not differentiate between an open tree structure and one in which there are interconnections between branches. Two such structures may have the same fractal dimension by virtue of their space-filling properties, but have widely different structures in their fluid dynamic design and function. A way of discussing fractal properties that is particularly suited to open tree structures and that is used in this paper is that of considering L-system models by which the tree can be generated.

Since its inception, L-system formalism has been used and validated as a tool. In plants, where it was first used, its power and utility was measured by its ability to generate the branching patterns of trees and bushes observed in nature. The test is a qualitative one, not quantitative, and the same approach is being used

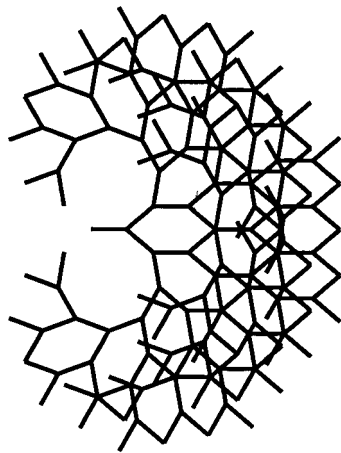
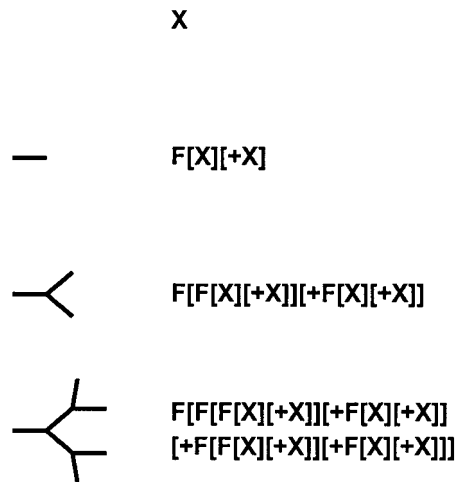


FIGURE 3. (top) The first four stages of a tree generated by system 1. The first X corresponds to the initial stage of production ($n = 1$), and since X has no graphical representation, it produces nothing in the left column. (bottom) The eighth stage of a tree generated by this L-system. The tree has the dichotomous branching pattern characteristic of arterial trees, but its uniformity is highly noncharacteristic of arterial trees.

in this paper. We look at whether known patterns in arterial branching can be mimicked by patterns produced within the confines of L-system formalism.

Basic L-System Branching Model

L-system formalism is particularly suited to open tree structures because it has a “grammar” especially developed for repeated branching. Although the formalism was originally developed for botanical structures, its language carries directly to arterial structures. Following that language and notation (Prusinkiewicz and Hanan, 1989; Prusinkiewicz and Lindenmayer, 1990), a basic L-system model for a tree structure consisting of repeated bifurcations, with axiom ω and production rule p , is given by:

$$\begin{aligned} \omega: & X \\ p: & X \rightarrow F[-X][+X], \end{aligned} \tag{1}$$

where F represents a line of unit length in the horizontal direction and X is an auxiliary symbol that has no graphical representation but plays an essential role in the branching process. The square brackets represent the departure from ($[$) and return to ($]$) a branch point, whereas the plus and minus signs represent turns through a given angle δ in the clockwise and anticlockwise directions, respectively. The first four stages of a tree produced by this system, denoted by $n = 1-4$, are then given by:

$$\begin{aligned} n = 1 & X \\ n = 2 & F[-X][+X] \\ n = 3 & F[-F[-X][+X]][+F[-X][+X]] \\ n = 4 & F[-F[-F[-X][+X]][+F[-X][+X]]] \\ & [+F[-F[-X][+X]][+F[-X][+X]]], \end{aligned} \tag{2}$$

and the results are shown graphically in Fig. 3. Note that the tree is perfectly symmetrical and has uniform properties. Asymmetry and variable properties are introduced later.

Fractal Character

The fractal character of the tree produced in the previous section is evident by the fact that its growth from one stage to the next is achieved by the same production rule, namely that defined by p in system 1. It is also evident by the self-similarity of the tree structure, namely the fact that any subtree taken from the tree as a whole has the same (dichotomous branching) structure as the whole. This self-similarity property can be expressed more rigorously within the L-system formalism by adopting a somewhat different L-system model for generating the tree, namely:

$$\begin{aligned} \omega: & F \\ p: & F \rightarrow F[-F][+F]. \end{aligned} \tag{3}$$

The first four stages of the tree are given by:

$$\begin{aligned} n = 1: & F \\ n = 2: & F[-F][+F] \\ n = 3: & F[-F][+F][-F[-F][+F]][+F[-F][+F]] \\ n = 4: & F[-F][+F][-F[-F][+F]][+F[-F][+F]] \\ & [-F[-F][+F][-F[-F][+F]][+F[-F][+F]]] \\ & [+F[-F][+F][-F[-F][+F]][+F[-F][+F]]], \end{aligned} \tag{4}$$

and the results are shown in Fig. 4. An important difference between this L-system and that of the previous section is that the production rule here, although producing the same tree structure as that produced by system 1, involves graphical duplication of some branch segments at each production beyond $n = 2$. At $n = 1$, the first junction point is produced and thereafter the graphical “turtle” always returns to that point after tracing each of the two sides of the tree arising from that junction. If each of the duplications is treated as an overwriting of the existing segment, then the resulting tree is graphically the same as that produced by system 1.

An important advantage of this system, however, is that it provides a more explicit expression of the self-similarity property of the tree by making it possible to define any stage of the tree as an axiom, and then applying the same production rule to that axiom to produce the tree. In particular, taking the second stage of the tree in system 4 as an axiom, we obtain the following system:

$$\begin{aligned} B & \equiv F[-F][+F] \\ \omega: & B \\ p: & B \rightarrow B[-B][+B]. \end{aligned} \tag{5}$$

The first three stages of the tree are given by:

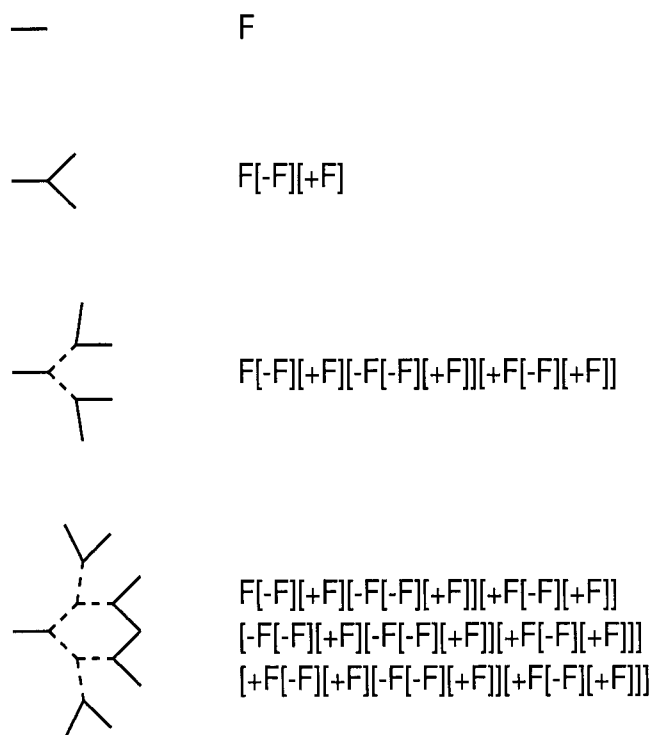


FIGURE 4. The first four stages of the modified structure defined in system 3. The dashed segments in stages 3 and 4 indicate segments where duplication or “overwriting” has occurred.

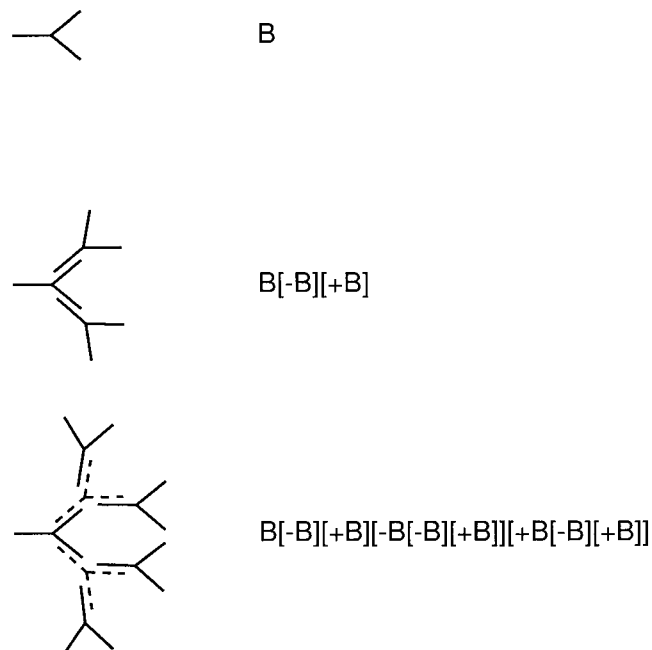


FIGURE 5. The first three stages of the modified structure defined in system 5, where a subtree B is used as an axiom instead of the basic line step F . Production steps can be seen to proceed only in terms of B (not F), as illustrated schematically in the second and third stage. As before, the dashed units refer to duplication or overwriting. The branches are displaced sideways from each other only to make them graphically visible.

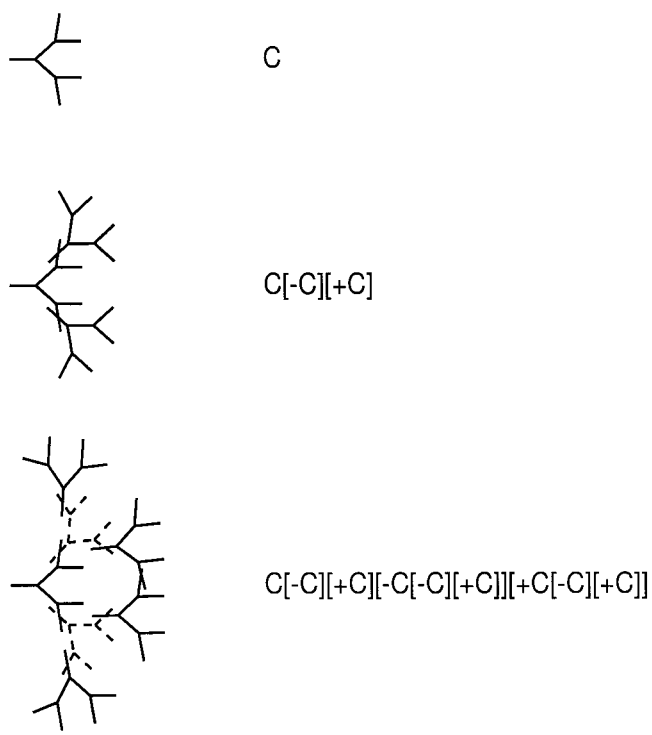


FIGURE 6. The first three stages of the modified structure defined in system 7 where a subtree C is used as an axiom instead of the basic line step F . Production steps can be seen to proceed only in terms of C (not F), as illustrated schematically in the second and third stage. As before, the dashed units refer to duplication or overwriting. The branches are displaced sideways from each other only to make them graphically visible.

$$\begin{aligned}
 n = 1: & \quad B \\
 n = 2: & \quad B[-B][+B] \\
 n = 3: & \quad B[-B][+B][-B[-B][+B]][+B[-B][+B]],
 \end{aligned}
 \tag{6}$$

and the results are shown in Fig. 5. Similarly, taking the third stage of the tree in system 4 (or the second stage of the tree in system 6) as an axiom, we obtain the following system:

$$\begin{aligned}
 B & \equiv F[-F][+F] \\
 C & \equiv B[-B][+B]
 \end{aligned}
 \tag{7}$$

$$\begin{aligned}
 \omega: & \quad C \\
 p: & \quad C \rightarrow C[-C][+C].
 \end{aligned}$$

The first three stages of the tree are now given by:

$$\begin{aligned}
 n = 1: & \quad C \\
 n = 2: & \quad C[-C][+C] \\
 n = 3: & \quad C[-C][+C][-C[-C][+C]][+C[-C][+C]],
 \end{aligned}
 \tag{8}$$

and the results are shown in Fig. 6. Comparison of the three L-systems shows that the production rules in systems 5 and 7 are identical in form to the production rule in system 3. Indeed, this bracketed form is the generator of dichotomy in the three cases.

The key difference between these two systems and that of the previous section is that production here proceeds in terms of B or C without any reference back to F once the symbols B and C have been defined. This feature is illustrated graphically in Figs. 5 and 6. The lowest building unit here is not F but B or C as the

case may be and as illustrated in these figures. The fact that B or C can be any stage of the tree while the production rule remains unchanged provides an algorithmic expression of self-similarity and of fractal character. This rather elegant expression of self-similarity is not possible with system 1 since, in that system, F continues to appear explicitly in the production rule.

Although system 3 has the problem of duplication or overwriting of branch segments as discussed earlier, this is balanced by the advantage that production here can be “speeded up” considerably by taking a larger and larger subtree as axiom. This can have significant advantage both graphically, as illustrated in Figs. 5 and 6, and algorithmically. Indeed, in terms of F , the algorithmic expression for the third stage of the tree in system 8 would be the following:

$$\begin{aligned}
 n = 3: & \quad F[-F][+F][-F[-F][+F]][+F[-F][+F]] \\
 & \quad [-F[-F][+F][-F[-F][+F]][+F[-F][+F]]] \\
 & \quad [+F[-F][+F][-F[-F][+F]][+F[-F][+F]]] \\
 & \quad [-F[-F][+F][-F[-F][+F]][+F[-F][+F]]] \\
 & \quad [-F[-F][+F][-F[-F][+F]][+F[-F][+F]]] \quad (9) \\
 & \quad [+F[-F][+F][-F[-F][+F]][+F[-F][+F]]] \\
 & \quad [+F[-F][+F][-F[-F][+F]][+F[-F][+F]]] \\
 & \quad [-F[-F][+F][-F[-F][+F]][+F[-F][+F]]] \\
 & \quad [+F[-F][+F][-F[-F][+F]][+F[-F][+F]]]
 \end{aligned}$$

compared with the much simpler expression in terms of C in system 8.

Elements of Arterial Branching

As stated earlier, arterial trees have been found to consist of primarily dichotomous branching, the basic structural unit of the tree being an arterial “bifurcation,” whereby an arterial segment divides into two branches and then each of the branches goes on to do the same, and so on (Zamir and Brown, 1982). If the diameter and length of an arterial segment are denoted by d , and l , respectively, and if at an arterial bifurcation subscripts 0, 1, and 2 are used to identify the parent segment and its two branches, then the basic properties at that bifurcation are d_0, d_1, d_2 and l_0, l_1, l_2 , as shown schematically in Fig. 7. Another two important properties

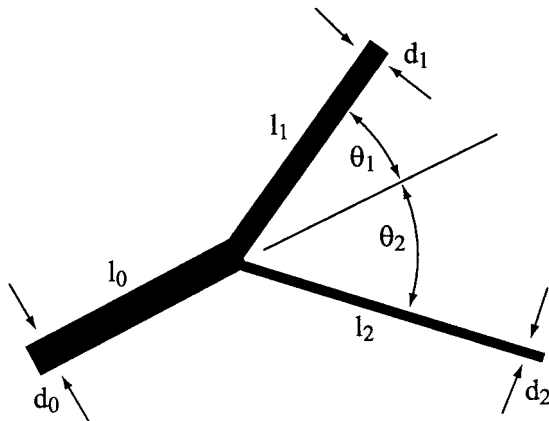


FIGURE 7. The basic variables at an arterial bifurcation are the lengths and diameters of the three vessel segments involved, and the angles that the two branches make with the direction of the parent vessel. In this paper, the convention is used that subscript 1 always refers to the branch with the larger diameter, and in graphical constructions that branch is always placed at an angle in an anticlockwise direction from that of the parent vessel. The convention is purely arbitrary, but it has a bearing on the “slant” of non-symmetrical trees constructed in this way.

are the angles θ_1 and θ_2 , which the two branches make with the direction of the parent segment (Fig. 7). In what follows, the convention is used that all properties with subscript 1 refer to the branch with the larger diameter, i.e., the inequality $d_1 > d_2$ is always assumed to apply, except, of course, when the two branch diameters are equal. This allows the definition of a useful parameter, sometimes referred to as the bifurcation index or asymmetry ratio:

$$\alpha = \frac{d_2}{d_1}, \quad (10)$$

which has the convenient range of values 0–1.0. The index is a measure of the asymmetry of the two diameters at an arterial bifurcation, with $\alpha = 1.0$ when the two diameters are equal, and $\alpha \approx 0$ when one of the two diameters is very much larger than the other.

One of the most fundamental laws underlying the structure of arterial trees is that relating the diameter d of an arterial segment to the flow rate q , which the segment is destined to carry. A classical result obtained by Murray (1926a) prescribes a “cube law” relationship, namely $q \propto d^3$. The result is based on a compromise between the power required to drive steady flow through the vessel, which varies as d^{-4} , and the rate of expenditure of metabolic energy required to maintain the volume of blood filling the vessel, which varies as d^2 . Data from the cardiovascular systems of humans and animals have given the law considerable support, though with a great deal of scatter (Rodbard, 1975; Hutchins et al., 1976; Mayrovitz and Roy, 1983). Other power laws of the form $q \propto d^k$ have been considered, with values of k different from three (Sherman, 1981; Roy and Woldenberg, 1982; Woldenberg and Horsfield, 1983). There are some indications that at the higher end of the arterial tree, the value of k is close to two, whereas in the core of the tree and the precapillary end it is close to three (Zamir et al., 1992; West et al., 1997). However, a clear picture has not been established because the scatter in physiological data makes it difficult to distinguish accurately between the two. Nevertheless, many theoretical studies continue to be based on the cube law because of its clear theoretical basis and because it has been tested widely against physiological data. For the same reasons, the cube law is used in this paper to provide the required parameters for L-system algorithms. A different power law can be used instead, in a fairly straightforward manner.

Application of the cube law at an arterial bifurcation provides the basis for its role in arterial branching. Conservation of flow rate at an arterial bifurcation requires that flow rate in the parent vessel equals the sum of flow rates in the two branches (Fig. 7), i.e., $q_0 = q_1 + q_2$. Application of the cube law then converts this into a relation between the diameters of the three vessels, namely $d_0^3 = d_1^3 + d_2^3$, and the following two diameter ratios can then be defined in terms of α :

$$\lambda_1 = \frac{d_1}{d_0} = \frac{1}{(1 + \alpha^3)^{1/3}}, \quad \lambda_2 = \frac{d_2}{d_0} = \frac{\alpha}{(1 + \alpha^3)^{1/3}}. \quad (11)$$

Another important parameter is the ratio γ of branch length to the length of the parent vessel at an arterial bifurcation. So far, there have been no theoretical grounds for determining this ratio, but biological data indicate that the length of a vessel segment is very weakly related to its diameter in the sense that vessel segments of smaller diameter tend to have smaller lengths, though exceptions occur in sufficiently large number to blur any consistent relation. At best, the data suggest a maximum length to diameter ratio of ~ 35 and an approximate average of 10 (Zamir, 1999). Using this average value for the present purpose, values of γ for the two branches in an arterial bifurcation are then equal to the corresponding values of the diameter ratios, namely

$$\gamma_1 = \frac{l_1}{l_0} = \frac{d_1}{d_0} = \lambda_1, \quad \gamma_2 = \frac{l_2}{l_0} = \frac{d_2}{d_0} = \lambda_2. \quad (12)$$

Finally, to complete the structure of an arterial bifurcation, it is necessary to define the angles, θ_1 and θ_2 , that the two branches make with the direction of the parent vessel (Fig. 7). There are optimum values of these angles that minimize the total volume of the three vessel segments, given by Murray (1926b) and Zamir (1978):

$$\begin{aligned} \cos \theta_1 &= \frac{(1 + \alpha^3)^{4/3} + 1 - \alpha^4}{2(1 + \alpha^3)^{2/3}}, \\ \cos \theta_2 &= \frac{(1 + \alpha^3)^{4/3} + \alpha^4 - 1}{2\alpha^2(1 + \alpha^3)^{2/3}}. \end{aligned} \quad (13)$$

Combined with the cube law, the same angles also minimize the pumping power required to drive the flow through the bifurcation. It can be observed from these expressions that, in a non-symmetrical bifurcation ($\alpha < 1.0$), the branch with the larger diameter makes a smaller branching angle than does the other branch, i.e., $\theta_1 < \theta_2$.

Parametric L-System Branching

The variables of arterial branching λ , γ , θ_1 , and θ_2 , can be incorporated into the L-system formalism by using a so-called "parametric L-system" (Prusinkiewicz and Lindenmayer, 1990) that would embody these variables. The first two variables are introduced by using a two-parameter step function $F(L, W)$ in which L represents a step length and W represents a step width. Then, in an arterial tree, L is taken to represent the length of a vessel segment, and W is taken to represent the diameter of that segment.

The branching angles are introduced by using one-parameter rotation functions $+(\delta_1)$ and $-(\delta_2)$ in which the angles of clockwise and anticlockwise rotations are stated explicitly and individually through the values of δ_1 and δ_2 .

The basic parametric L-system for a dichotomous tree then takes the form:

$$\begin{aligned} \omega: & X(L, W) \\ p: & X(L, W) \rightarrow F(L, W)[-(\delta_1)X(L, W)][+(\delta_2)X(L, W)], \end{aligned} \quad (14)$$

where the tree production now requires that values of the parameters L , W , δ_1 , and δ_2 be specified. In fact, the basic L-systems considered in previous sections also require these values, but when the parameters are not included explicitly in the algorithm, as in previous sections, it is assumed that their values are fixed throughout the tree structure. Indeed, in the trees shown in Figs. 3–6, the values $L = 1$, $W = 1$, and $\delta_1 = \delta_2 = 40^\circ$ were implicitly used, though not stated. Also, it is convenient, particularly for computer-generated images, to allow the scales of L and W to be different from each other. In this way, $L = 1$, $W = 1$ above can be taken to mean that L is one unit of length (in centimeters, for example) while W is one unit of width (e.g., in millimeters); thus, the unit of length being different from the unit of width.

One of the most powerful features of parametric L-systems is that the values of these parameters can be changed along a tree structure, and the pattern of that change can be incorporated into the production algorithm. This makes it possible to make branches smaller than parents, both in length and diameter, and

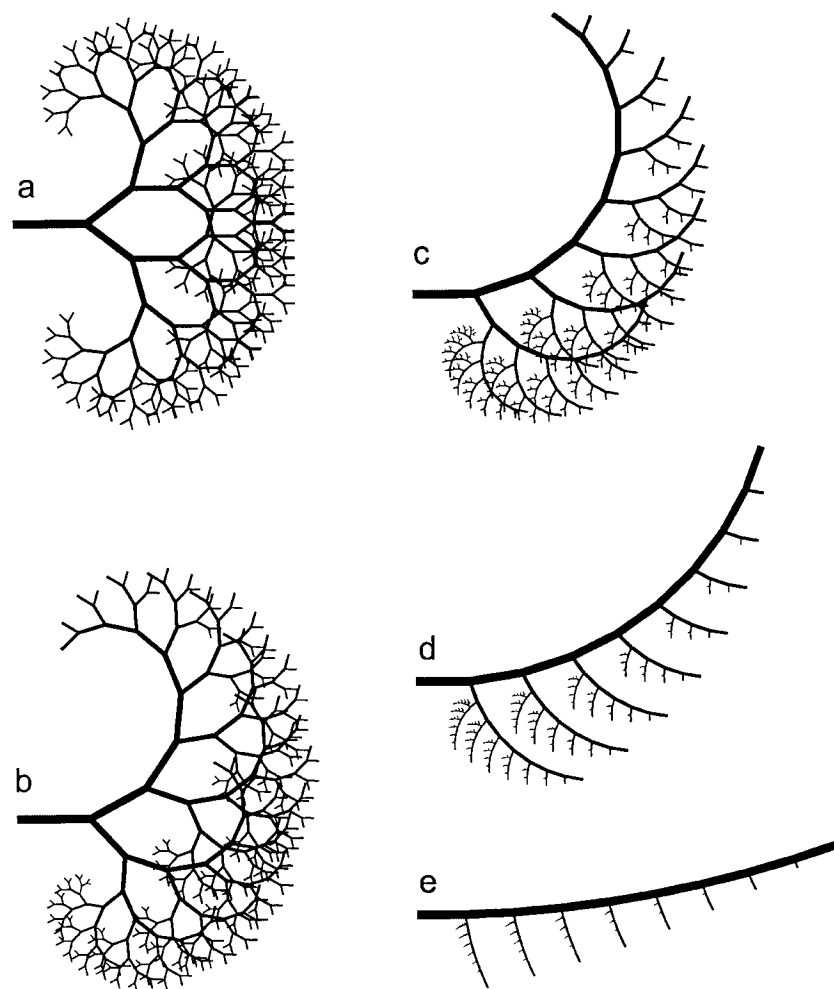


FIGURE 8. The ninth stage of tree structures generated by system 15, with the parameters being determined by the value of the bifurcation index α , which is a measure of asymmetry of the bifurcations that make up the tree. (a) $\alpha = 1.0$, which corresponds to perfectly symmetrical bifurcations; (b) $\alpha = 0.8$; (c) $\alpha = 0.6$; (d) $\alpha = 0.4$; and (e) $\alpha = 0.2$. Although α is constant in each tree, the lengths and diameters of branches diminish as the tree progresses.

to give branches individual branching angles. These changes can be made consistent with the characteristics of arterial branching discussed in the previous section by taking,

$$\begin{aligned} \omega: & X(L_0, W_0) \\ p: & X(L, W) \rightarrow F(L, W)[-(\theta_1)X(\gamma_1 L, \lambda_1 W)][+(\theta_2)X(\gamma_2 L, \lambda_2 W)]. \end{aligned} \quad (15)$$

It should be noted that although X is only an auxiliary symbol that has no graphical interpretation, it must nevertheless carry the parameters prescribed by the production rule because these become the parameters of the branches in the next production cycle. Values of L_0, W_0 in the axiom represent the length and width of the first line segment that must be specified. The lengths and widths of subsequent line segments are then adjusted by the scaling parameters $\gamma_1, \gamma_2, \lambda_1,$ and λ_2 , and their branching angles are determined by θ_1 and θ_2 . The scaling occurs at each production cycle, and is therefore compounded as production progresses. This can be observed by writing down the first three stages of the tree, namely

$$\begin{aligned} n = 1: & X(L_0, W_0) \\ n = 2: & F(L_0, W_0)[-(\theta_1)X(\gamma_1 L_0, \lambda_1 W_0)][+(\theta_2)X(\gamma_2 L_0, \lambda_2 W_0)] \\ n = 3: & F(L_0, W_0) \\ & [-(\theta_1)F(\gamma_1 L_0, \lambda_1 W_0)[-(\theta_1)X(\gamma_1^2 L_0, \lambda_1^2 W_0)][+(\theta_2)X(\gamma_2^2 L_0, \lambda_2^2 W_0)]] \\ & [+(\theta_2)F(\gamma_2 L_0, \lambda_2 W_0)[-(\theta_1)X(\gamma_1^2 L_0, \lambda_1^2 W_0)][+(\theta_2)X(\gamma_2^2 L_0, \lambda_2^2 W_0)]. \end{aligned} \quad (16)$$

It is to be recalled that, by convention, the parameters $\gamma_1, \lambda_1,$ and θ_1 at each bifurcation are associated with the branch that has the larger diameter, whereas $\gamma_2, \lambda_2,$ and θ_2 are associated with the branch that has the smaller diameter. Furthermore, in the above systems (15 and 16), the angle θ_1 has been associated with an anticlockwise turn (minus sign), whereas the angle θ_2 has been associated with a clockwise turn (plus sign). As a result of these conventions, the branch with the larger diameter at a bifurcation will always appear on the same side of the parent vessel, namely at an anticlockwise angle. These conventions are purely arbitrary, and can be reversed or changed in a number of ways. The conventions do affect the orientation and appearance of a tree structure, however, and must therefore be recalled when interpreting the resulting tree structure.

Finally, since the scaling parameters $\gamma_1, \lambda_1, \gamma_2,$ and λ_2 and branching angles θ_1 and θ_2 are all functions of the bifurcation index α (Eqs. 11–13), the above system 15 will generate a different arterial tree for each value of α . For $\alpha = 1.0$, all bifurcations are symmetrical and so is the resulting tree structure (Fig. 8 a), although the lengths and diameters of vessel segments are diminishing in accordance with the rules of arterial branching. The effect of small asymmetry is shown in Fig. 8 b, where $\alpha = 0.8$, and the results for $\alpha = 0.6, 0.4,$ and 0.2 are shown in Fig. 8, c–e.

DISCUSSION AND CONCLUSIONS

Results in Fig. 8 (a–e) demonstrate clearly that parametric L-systems can generate a wide spectrum of tree structures that have the theoretical properties of arterial branching and that, by construction, have a fractal pattern.

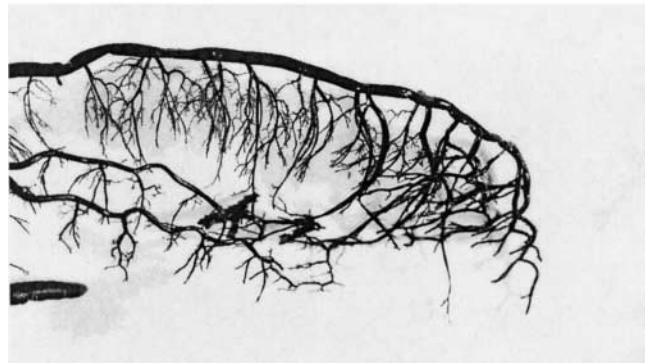
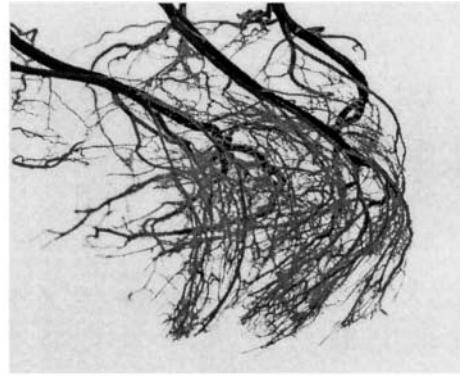


FIGURE 9. (top) Coronary arteries of the “delivering” type that typically enter the myocardium and branch profusely to reach the capillary bed (Zamir, 1988). In this type of branching, the vessels rapidly lose their identity as their diameters diminish rapidly. (bottom) A coronary artery of the “distributing” type that typically circles the heart as it gives rise to branches. In contrast with the pattern observed above, here the vessel retains its diameter and identity through a considerable number of branching sites.

At one end of this spectrum is a tree with symmetrical bifurcations ($\alpha = 1.0$) in which the diameters of vessel segments diminish rapidly as the tree structure progresses (Fig. 8 a). At symmetrical bifurcations, the diameter reduction ratios λ_1 and λ_2 are equal and have their maximum value of 0.794 (Eq. 11), i.e., vessel diameters are reduced by $\sim 20\%$ at each bifurcation. In this case, the tree progresses most “rapidly” toward its ultimate level at which the branches implement the delivery of blood to the capillary bed. Vessels with this branching pattern have been termed “delivering vessels” (Zamir, 1988; Pollanen, 1992). In the coronary circulation, they are the vessels that enter the depth of the myocardium and branch profusely to reach the capillary bed (Fig. 9, top).

At the other end of the spectrum, is a tree with highly nonsymmetrical bifurcations ($\alpha \approx 0$) in which the diameter of the leading branch at each bifurcation is only slightly reduced. In Fig. 8 e, where $\alpha = 0.2$, and hence from Eq. 11 $\lambda_1 \approx 0.997$, the reduction is only 0.3%. In this case, the leading artery retains its identity and much of the flow rate that it carries as the tree progresses. Ves-

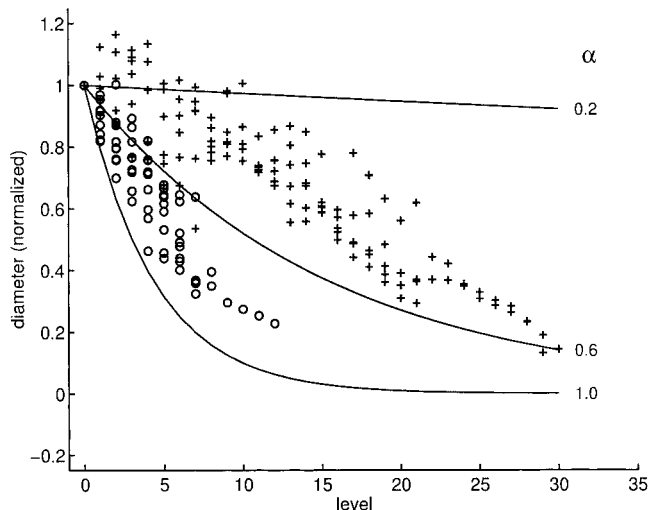


FIGURE 10. Quantitative comparison of the delivering (○) and distributing (+) patterns of branching in Fig. 9. The data points show measured diameters at different levels of the branching tree structure of vessels of the two types (Zamir, 1988). The solid curves represent the diameter progression along three of the L-system trees in Fig. 8 ([Fig. 8 a] $\alpha = 1.0$; [Fig. 8 c] $\alpha = 0.6$; and [Fig. 8 e] $\alpha = 0.2$). It is observed that although the diameter progression along the physiological trees is not characterized by a single curve that corresponds to a single value of the asymmetry ratio α , there is a clear preponderance for higher values of α in one case and lower values in the other, thus identifying somewhat with the corresponding L-system trees.

sels with this pattern of branching have been termed “distributing vessels” (Zamir, 1988; Pollanen, 1992). In the coronary circulation, they have been identified as the main coronary arteries that circle the heart as they give rise to secondary branches (Fig. 9, bottom).

Thus, certain arterial branching patterns can be mimicked by fractal L-system trees, using an appropriate choice of branching parameters. However, the L-system trees have one important characteristic that is rarely shared by arterial trees in the cardiovascular system. In each panel of Fig. 8, the value of α is fixed throughout that particular tree structure (although values of the L-system parameters do change from one level of the tree to the next). This type of uniformity is rarely observed in the physiological system. The vasculature of the kidney shown in Fig. 2, for example, is like the fractal tree shown in Fig. 8 a in general appearance, but the first clearly lacks the uniformity inherent in the second. The primary source of this nonuniformity in arterial trees is the value of the bifurcation index α . Data from the vascular system have shown consistently that α takes on almost the full range of values (0–1.0) at each level of a tree and from one level to the next (Zamir, 1999). However, distinct patterns of branching such as those in Fig. 9 have been shown to have a preponderance for higher or lower values of α as shown in Fig. 10.

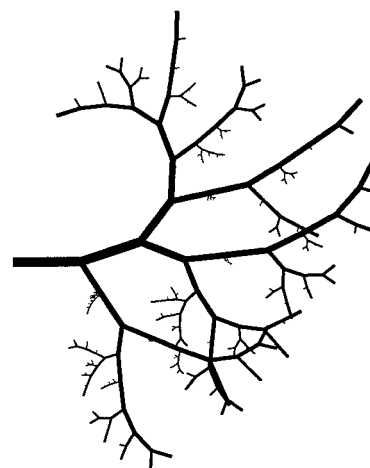
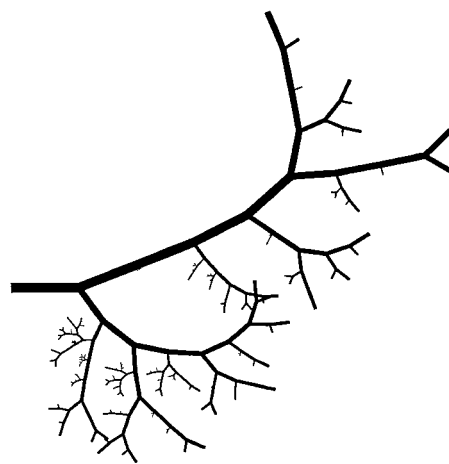


FIGURE 11. The ninth stage of two tree structures generated by system 15, but here the values of α on which parameters depend are assigned randomly at each bifurcation in the range 0–1.0.

Variability in the value of the asymmetry ratio, α , can be incorporated into the L-system by assigning a random value to α between 0 and 1.0 at each branch point. Two examples of the resulting trees are shown in Fig. 11, which raise two important questions. First, is the wide variability in the value of α observed in physiological data actually random, or is it determined by local conditions and other constraints that, therefore, cannot be modeled by purely random variation? Second, is it legitimate to refer to the trees in Fig. 11 and to arterial trees that they mimic as fractal structures? Although the trees in Fig. 11 are generated by an L-system in which the production rule has the same form at all levels of the tree, the values of the parameters involved are not predetermined. The second stage of one of the trees in Fig. 11, for example, cannot be used to generate the third and subsequent stages of that tree as was done in Figs. 5 and 6. Indeed, the second stage itself cannot be regenerated because it would be randomly different at each production.

The question of whether arterial trees have fractal structures has important bearing on the more general question of scaling in biology (Sernetz et al., 1985; West et al., 1997). It would seem, in conclusion, that parametric L-systems can be used to produce fractal tree structures that have some but not all the branching characteristics of arterial trees. The key issue is the value of the asymmetry ratio α . Although a constant value of α near 0 or 1.0 produce branching patterns that have been observed in the physiological system, a random choice of α does not produce the pattern of variability found in the physiological system.

In the analogous problem of botanical tree structures, probabilities have sometimes been used to determine the value or nature of a branching variable in the production process (Nishida, 1980; MacDonald, 1983; Prusinkiewicz and Hanan, 1989; Prusinkiewicz and Lindenmayer, 1990). In the present case, this would be equivalent to giving each value of α a certain probability of occurring at each branch point. Data from the cardiovascular system have so far not shown any basis for assigning such probabilities. The choice of random values of α at each branch point is at least consistent with the range of variability shown by the data from the cardiovascular system, even if in the physiological setting the source of that variability is not known. Here, the values of α may be influenced by local anatomy, local flow requirements, and other constraints, and therefore the variability may not be purely random. On the other hand, in the botanical situation, there are indications that probabilities may well play a role in the growth of tree structures (Nishida, 1980; MacDonald, 1983; Prusinkiewicz and Hanan, 1989; Prusinkiewicz and Lindenmayer, 1990). An important difference between botanical and arterial tree structures may indeed lie in the legitimacy of using probabilities in branching algorithms in the two cases.

This work was supported by the Natural Sciences and Engineering Research Council of Canada.

Submitted: 13 February 2001

Revised: 6 July 2001

Accepted: 9 July 2001

REFERENCES

Berry, M., and D. Pymm. 1981. Analysis of neural networks. In *Neural Communication and Control*. G. Szekely, editor. Pergamon, Oxford. 155–169.

Hutchins, G.M., M.M. Miner, and J.K. Boitnott. 1976. Vessel caliber and branch-angle of human coronary artery branch-points. *Circ. Res.* 38:572–576.

Horton, R.E. 1945. Erosional development of streams and their

drainage basins: hydrophysical approach to quantitative morphology. *Bull. Geol. Soc. Am.* 56:275–370.

MacDonald, N. 1983. *Trees and Networks in Biological Models*. John Wiley & Sons Inc., Chichester. 215 pp.

Mandelbrot, B.B. 1977. *Fractals: form, chance, and dimensions*. Freeman, San Francisco. 365 pp.

Mayrovitz, H.N., and J. Roy. 1983. Microvascular blood flow: evidence indicating a cubic dependence on arteriolar diameter. *Am. J. Physiol.* 245:H1031–H1038.

Moffat, D.B. 1979. The anatomy of the renal circulation. In *Renal Disease*. D. Black and N.F. Jones, editors. Blackwell, Oxford.

Murray, C.D. 1926a. The physiological principle of minimum work. I. The vascular system and the cost of blood volume. *Proc. Natl. Acad. Sci.* 12:207–214.

Murray, C.D. 1926b. The physiological principle of minimum work applied to the angle of branching of arteries. *J. Gen. Physiol.* 9:835–841.

Nishida, T. 1980. KOL-simulating almost but not exactly the same development. *Mem. Fac. Sci. Kyoto Univ. Ser. Biol.* 8:97–122.

Peitgen, H.O., H. Jurgens, and D. Saupe. 1992. *Chaos and Fractals: New Frontiers of Science*. Springer-Verlag, New York. 984 pp.

Pollanen, M.S. 1992. Dimensional optimization at different levels of the arterial hierarchy. *J. Theor. Biol.* 159:267–270.

Prusinkiewicz, P., and J. Hanan. 1989. *Lindenmayer Systems, Fractals, and Plants*. Lecture Notes in Biomathematics. Vol. 79. Springer-Verlag, New York. 120 pp.

Prusinkiewicz, P., and A. Lindenmayer. 1990. *The Algorithmic Beauty of Plants*. Springer-Verlag, New York. 228 pp.

Rodbard, S. 1975. Vascular caliber. *Cardiology*. 60:4–49.

Roy, A.G., and M.J. Woldenberg. 1982. A generalization of the optimal models of arterial branching. *Bull. Math. Biol.* 44:349–360.

Sernetz, M., B. Gelleri, and F. Hofman. 1985. The organism as a bioreactor, interpretation of the reduction law of metabolism in terms of heterogeneous catalysis and fractal structure. *J. Theor. Biol.* 117:209–230.

Sherman, T.F. 1981. On connecting large vessels to small. The meaning of Murray's Law. *J. Gen. Physiol.* 78:431–453.

Weibel, E.R. 1984. *The Pathways for Oxygen*. Harvard University Press, Cambridge, MA. 425 pp.

West, G.B., J.H. Brown, and B.J. Enquist. 1997. A general model for the origin of allometric scaling laws in biology. *Science*. 276:122–126.

Woldenberg, M.J., and K. Horsfield. 1983. Finding the optimal length for three branches at a junction. *J. Theor. Biol.* 104:301–318.

Zamir, M. 1978. Nonsymmetrical bifurcations in arterial branching. *J. Gen. Physiol.* 72:837–845.

Zamir, M. 1988. Distributing and delivering vessels of the human heart. *J. Gen. Physiol.* 91:725–735.

Zamir, M. 1999. On fractal properties of arterial trees. *J. Theor. Biol.* 197:517–526.

Zamir, M., and N. Brown. 1982. Arterial branching in various parts of the cardiovascular system. *Am. J. Anat.* 163:295–307.

Zamir, M., and S. Phipps. 1987. Morphometric analysis of the distributing vessels of the kidney. *Can. J. Physiol. Pharmacol.* 65:2433–2440.

Zamir, M., P. Sinclair, and T.H. Wonnacott. 1992. Relation between diameter and flow in major branches of the arch of the aorta. *J. Biomech.* 25:1303–1310.

Zamir, M., S.M. Wrigley, and B.L. Langille. 1983. Arterial bifurcations in the cardiovascular system of a rat. *J. Gen. Physiol.* 81:325–335.